

Constraints on sterile neutrino as a dark matter candidate from the diffuse X-ray background

A. Boyarsky^{1,5}, A. Neronov^{2,3}, O. Ruchayskiy⁴, M. Shaposhnikov⁵

¹ CERN, Theory department, Ch-1211 Geneve 23, Switzerland

² INTEGRAL Science Data Center, Chemin d'Écogia 16, 1290 Versoix, Switzerland

³ Geneva Observatory, 51 ch. des Maillettes, CH-1290 Sauverny, Switzerland

³ Institut des Hautes Études Scientifiques, Bures-sur-Yvette, F-91440, France

⁵ École Polytechnique Fédérale de Lausanne, Institute of Theoretical Physics, FSB/ITP/LPPC, BSP 720, CH-1015, Lausanne, Switzerland

Received <date> ; in original form <date>

ABSTRACT

Sterile neutrinos with masses in the keV range are viable candidates for the warm dark matter. We analyze existing data for the extragalactic diffuse X-ray background for signatures of sterile neutrino decay. The absence of detectable signal within current uncertainties of background measurements puts model-independent constraints on allowed values of sterile neutrino mass and mixing angle, which we present in this work.

1 INTRODUCTION

At present time there exists an extensive body of evidence that most of the matter in the Universe is composed of new, yet undiscovered particles – dark matter (DM). Observations of (i) galactic rotation curves, (ii) cosmic microwave background radiation, (iii) gravitational lensing, and (iv) X-ray emission of hot gas in galaxy clusters provide independent measurements of DM content of the Universe.

Another major experimental discovery of the recent decade is that of neutrino oscillations. There are separate measurements of neutrino oscillations in solar neutrinos (Ahmad et al. (2002)), atmospheric neutrinos (Fukuda et al. (1998)), and reactor neutrinos (Eguchi et al. (2003)). Neutrino oscillations can be explained if neutrino is a massive particle, contrary to the Standard Model assumption. This means that along with the usual left-handed (or *active*) neutrinos there may exist also right-handed or *sterile neutrinos*.

Conventional sea-saw mechanism (Minkowski (1977); Yanagida (1979;1980)); Gell-Mann et al. (1980); Ramond (1979); Mohapatra & Senjanovic (1980); Glashow (1980)) of generation of small active neutrino masses implies that the sterile neutrinos are heavy (usually of the order of GUT energy scale $\sim 10^{10} - 10^{15}$ GeV) and that their mixing with usual matter is of the order $\sin \theta \sim 10^{-10} - 10^{-15}$. In addition of the smallness of neutrino masses, models of this type can explain baryon asymmetry of the Universe via thermal leptogenesis (Fukugita & Yanagida (1986)) and anomalous electroweak fermion number non-conservation (Kuzmin et al. (1985)). However they do not offer a DM candidate.

Recently it was proposed that neutrino oscillations, the origin of the dark matter, and baryon asymmetry of the Universe can be consistently explained in the model called *neutrino Minimal Standard Model* (*vMSM*) (Asaka et al. (2005); Asaka & Shaposhnikov (2005)). This model is a natural extension of minimal Standard Model (MSM), where three right-handed neutrinos are introduced into the MSM Lagrangian. In this extension neutrinos obtain Dirac masses via Yukawa coupling analogous to the other quarks and leptons of MSM and in addition Majorana mass terms are allowed for

right-handed neutrinos. Unlike conventional see-saw scenarios, all of these Majorana masses (which are roughly equal to the masses of corresponding sterile neutrinos) are chosen such that the mass of the lightest sterile neutrino is in the keV range and the other ones are $\lesssim 100$ GeV — below electroweak symmetry breaking scale. In this model a role of the dark matter particle is played by the lightest sterile neutrino.

The existence of a relatively light sterile neutrino has non-trivial observable consequences for cosmology and astrophysics. It was noticed already in Olive & Turner (1982); Dodelson & Widrow (1993); Shi & Fuller (1999); Dolgov & Hansen (2002) that a sterile neutrino with the mass in the keV range appears to be a viable “warm” DM candidate. The small mixing angle ($\sin \theta \sim 10^{-6} - 10^{-4}$) between sterile and active neutrino ensures that sterile neutrinos were never in thermal equilibrium in the early Universe and thus allows their abundance to be smaller than the equilibrium one (Dodelson & Widrow (1993)). Moreover, a sterile neutrino with these parameters is important for the physics of supernova (Fryer & Kusenko (2005)) and can explain the pulsar kick velocities (Kusenko & Segre (1997); Fuller et al. (2003); Barkovich et al. (2004)).

In addition to the dominant decay mode into three active neutrinos, the light (with mass $m_s \lesssim 1$ MeV) sterile neutrino can decay into an active one and a photon with the energy $E_\gamma = m_s/2$. Thus, there exists a possibility of direct detection of neutrino decay emission line from the sources with big concentration of DM, e.g. from the galaxy clusters (Abazajian et al. (2001b)). Similarly, the signal from radiative sterile neutrino decays accumulated over the history of the Universe could be seen as a feature in the diffuse extragalactic background light spectrum. This opens up a possibility to study the physics beyond the Standard Model using astrophysical observations.

Recently there has been a number of works devoted to the analysis of the possibility to discover sterile neutrino radiative decays from X-ray observations (Abazajian et al. (2001b); Viel et al. (2005); Mapelli & Ferrara (2005)). For example, it was argued by (Abazajian et al. (2001b)) that if sterile neutrinos composed 100%

of all the DM, one should be able to detect the DM decay line against the background of the X-ray emission from the Virgo cluster. According to Abazajian et al. (2001b) the non-detection of the line puts an upper limit $m_s < 5$ keV on the neutrino mass (this limit was, however recently revised in Abazajian (2005), who finds the restriction $m_s < 8$ keV). It was also noted by (Abazajian et al. (2001b); Mapelli & Ferrara (2005)) that one can obtain even stronger constraints $m_s \lesssim 2$ keV – from diffuse extragalactic X-ray background (XRB) under the assumption, that the dark matter in the Universe is uniformly distributed up to the distances, corresponding to red shifts $z \ll 1$. Together with the claim of Viel et al. (2005), putting lower bound $m_s > 2$ keV on the neutrino mass from Lyman α -forest observations, this would lead to a very narrow window of allowed sterile neutrino masses, if not exclude it completely.

In this paper we re-analyze the limit imposed on the parameters of sterile neutrino by the observations of the diffuse X-ray background (XRB). For that we are processing actual astrophysical data of HEAO-1 and XMM-Newton missions. There are several motivations for this. Namely

(i) All the above restrictions on sterile neutrino mass (Abazajian et al. (2001b); Dolgov & Hansen (2002); Mapelli & Ferrara (2005); Abazajian (2005)) are model dependent and based on the assumption that sterile neutrinos were absent in the early Universe at temperatures larger than few GeV. Depending on the model, the relation between the mass of sterile neutrino, the mixing angle and the present-day sterile neutrino density Ω_s does change. In fact, to compute the sterile neutrino abundance one needs to know whether there is any substantial lepton asymmetry of the universe at the time of sterile neutrino production, what is the coupling of sterile neutrino to other particles such as inflaton or super-symmetric particles, etc¹. Moreover, even if these uncertainties were removed, the reliable computation of the relic abundance of sterile neutrinos happens to be very difficult as the peak of their production falls on the QCD epoch of the universe evolution, corresponding to the temperature ~ 150 MeV (Dodelson & Widrow (1993)), where neither quark-gluon nor hadronic description of the plasma is possible. Therefore, before the particle physics model is fully specified and the physics of hadronic plasma is fully understood, one can not put a robust restriction on one single parameter of the model such as m_s .

Therefore we aim in this paper at clear separation between the model independent predictions, based solely on astrophysical observations and any statements that depend on a given model and underlying assumptions. To this end we treat m_s and $\sin \theta$ as two *independent* parameters and present the limits in the form of an “exclusion plot” in the $(m_s; \Omega_s \sin^2 \theta)$ parameter space.

It should be stressed that our data analysis is not based on any specific model of sterile neutrinos and as such can be applied to any “warm” DM candidate particle which has a radiative decay channel. In case of sterile neutrino the full decay width of this process is related to parameter $\sin \theta$ via Eq. (4) (see below).

(ii) Contrary to the previous works (Abazajian et al. (2001b); Mapelli & Ferrara (2005)), we argue that non-isotropy or “clumpiness” of the matter distribution in the nearby Universe *does not* relax the limit on the neutrino mass. Indeed, the fact that significant part of the dark matter at red shifts $z \lesssim 10$ is concentrated in galaxies and clusters of galaxies just means that the strongest signal

¹ For example, if the coupling of sterile neutrino to inflaton is large enough, the main production mechanism will be the creation of sterile neutrinos in inflaton oscillations rather than active-sterile neutrino transition.

from the dark matter decay should come from the sum of the signals from the compact sources at $z \lesssim 10$. Taking into account that DM decay signal from $z \lesssim 10$ is some 2 orders of magnitude stronger than that of from $z \gtrsim 10$, while the subtraction of resolved sources reduces the residual X-ray background maximum by a factor of 10, we argue that it would be wrong to subtract the contribution from the resolved sources from the XRB observations when looking for the DM decay signal. The form of XRB background spectrum with sources subtracted is, in fact, unknown and the assumption that it has a shape of initial spectrum, scaled down according to resolved fraction (as in Abazajian et al. (2001b)) requires additional justification.

(iii) We find that more elaborate analysis of the data enables to put tighter limits on the allowed region of the parameter space $(m_s, \Omega_s \sin^2 \theta)$ from the XRB observations. The idea is that the cosmological DM decay spectrum is characterized not only by the total flux but also by a characteristic shape (which depends on cosmological model). Assuming that the XRB spectrum is composed, in general, of a broad continuum of astrophysical origin and of the DM decay component, one can find that adding the DM decay component in a wrong place results in decrease of the overall quality of the fit of the data by the above two-component model (increase of the χ^2 of the fit). The condition that the two-component model provides an acceptable fit to the data imposes an upper limit on the flux in the DM decay component which is much more restrictive than the limit following from the condition that the flux of the DM component should not exceed the flux in the continuum component.

The paper is organized as follows. In Section 2 we compute the contribution of the radiative decay of sterile neutrino to the diffuse X-ray background (XRB) and compare its shape with that of measured XRB. We discuss the effects of non-uniformness of the DM distribution in Section 2.1. In Section 3 we obtain a model-independent exclusion region from HEAO-1 and XMM-Newton observations.

2 THE CONTRIBUTION OF DM DECAYS INTO THE XRB.

The sterile neutrino with a decay width Γ and mass m_s decays into an active neutrino and emits photons with a line-like spectrum at the energy $E_\gamma = m_s/2$. However, photons emitted at different cosmological distances are redshifted on their way to the Earth so that as a result the photon spectrum is given by (see Masso & Toldra (1999); Abazajian et al. (2001b)):

$$\frac{d^2N}{d\Omega dE} = \frac{\Gamma n_{DM}^0}{4\pi} \frac{1}{EH(m_s/(2E) - 1)}. \quad (1)$$

Here n_{DM}^0 is the DM number density at the present time and $H(z)$ is the Hubble parameter as a function of red shift. The explicit form of $H(z)$ depends on the cosmological parameters. This means that the expected dark matter decay spectrum is different for different cosmologies. For small z , $H(z)$ can be written as

$$H(z) \simeq H_0 \sqrt{\Omega_\Lambda + \Omega_{matter}(1+z)^3} \quad (z \ll 1), \quad (2)$$

where H_0 is the present-day value of the Hubble parameter and $\Omega_\Lambda, \Omega_{matter}$ are the cosmological constant and matter contributions to the density of the Universe. Substituting (2) into (1) we find that for small z the spectrum is approximated as

$$\frac{d^2N}{d\Omega dE} \simeq \frac{\Gamma n_{DM}^0}{2\pi H_0} \frac{(2E)^{1/2}}{\sqrt{8E^3\Omega_\Lambda + \Omega_{matter}m_s^3}}. \quad (3)$$

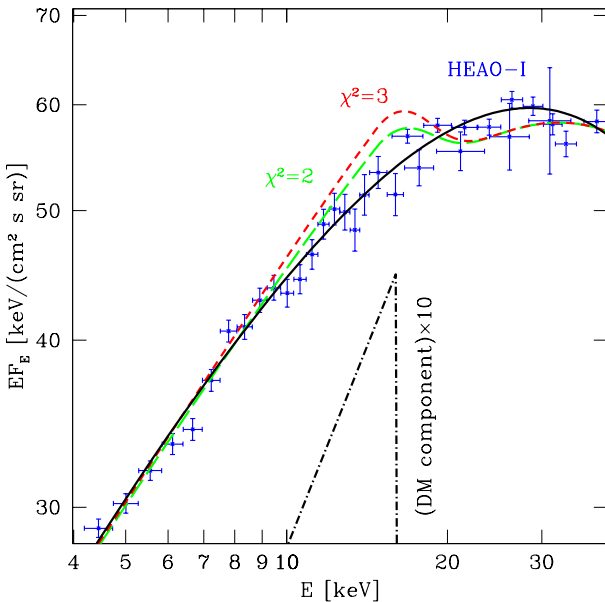


Figure 1. Diffuse X-ray background spectrum from HEAO-1 mission. The black solid curve shows empirical fit Eq. (5) by Gruber et al. (1999). The reduced χ^2 of this fit is 1.2. Dashed (green and red) lines represent the result of fit of the same data to the model of the form (5) with added DM component. The DM decay component (dot-dashed curve) is calculated for the “concordance” model $\Omega_\Lambda = 0.7$, $\Omega_{matter} = 0.3$ and for $m_s = 36.5$ keV. The green (long dashed) line represents a fit of DM with the mixing angle $\sin^2 2\theta = 1.9 \cdot 10^{-12}$ and the best achievable fit has the reduced $\chi^2 = 2$. For the red (short-dashed) line the mixing angle is $\sin^2 2\theta = 2.4 \cdot 10^{-13}$ and reduced $\chi^2 = 3$, which we choose as a border line of allowed quality of fit.

Assuming the Majorana nature of neutrino mass, the decay width Γ is related to $\sin \theta$ via (Dolgov & Hansen (2002))²:

$$\Gamma = \frac{9\alpha G_F^2}{256\pi^4} \sin^2 \theta m_s^5 = 5.6 \times 10^{-22} \sin^2 \theta \left(\frac{m_s}{1 \text{ keV}} \right)^5 \text{ sec}^{-1}. \quad (4)$$

As an example we show on Fig. 1 the expected dark matter decay spectrum for the cosmological “concordance” model with $\Omega_\Lambda \approx 0.7$, $\Omega_{matter} \approx 0.3$. One can see that close to the maximum the spectrum is roughly a power-law with the photon index equal to 1 ($dN/dE \sim E^{-1}$).

The measurements of the diffuse XRB (Marshal et al. (1980); Gruber et al. (1999)) show that for $3 \lesssim E \lesssim 60$ keV its form is well approximated by the following analytical expression

$$\frac{d^2 F_{XRB}}{dE d\Omega} = C_{XRB} \exp\left(-\frac{E}{T_{XRB}}\right) \left[\frac{E}{60 \text{ keV}} \right]^{-\Gamma_{XRB}+1} \frac{\text{keV}}{\text{keV} \cdot \text{sr} \cdot \text{sec} \cdot \text{cm}^2}. \quad (5)$$

In Fig. 1 we show the HEAO-1 data points³ together with the above analytical fit (solid black line). Such a form of XRB spectrum can be explained by AGN emission, under certain assumptions about AGN populations (Worsley et al. (2005); Treister & Urry (2005)). Below ~ 15 keV XRB was measured by many X-ray missions and the background was found to follow the power-law with the photon index $\Gamma_{XRB} \approx 1.3 - 1.4$ (Gruber et al. (1999); Lumb et al. (2002);

² Notice the factor of 2 difference between this reference and Eq. (4).

³ We thank D. Gruber for sharing this data with us and for many useful comments.

Revnivtsev et al. (2003, 2004); Gilli (2003); Barger (2003)). Analysis of Gruber et al. (1999) also finds $T_{XRB} = 41.13$ keV and $C_{XRB} = 7.9$. The DM decay component produces a harder spectrum, as one can see from Fig. 1.

2.1 The uniformness of the DM density in the Universe

Most of the power in the very hard DM decay spectrum of Fig. 1 is emitted in the narrow energy interval close to the maximal energy $E_{max} \approx m_s/2$. From Eq. (3) one can see that emission in this energy range is produced by neutrinos decaying at the present epoch ($z \approx 0$). For the case of the “concordance” model, the DM decay spectrum is characterized by the very hard inverted power law $dN/dE \sim E^{1/2}$ below the energy $\sim E_{max}/2$. The energy flux drops by an order of magnitude at the energies $\sim E_{max}/4$ which correspond to the redshift $z \approx 3$. Thus, most of the DM decay signal is collected from the low redshifts.

It is known that the process of structure formation leads to significant clustering of the dark matter at small redshifts. The signal from DM decays at small z is thus dominated by the sum of contributions from the point-like sources corresponding to the large DM concentrations, like galaxies or clusters of galaxies.

Abazajian et al. (2001b) and Mapelli & Ferrara (2005) argued that the clustering of the DM at small redshifts makes it difficult for the instruments that measure the diffuse X-ray background to detect the signal from the DM decays at small redshifts. Indeed, measurements of the diffuse X-ray background done with narrow-field instruments, like Chandra or XMM-Newton can miss the DM signal because of the absence of large nearby galaxies or galaxy clusters in the fields used for the deep observations and background measurements. As a measure for galaxy clustering one can take the distribution of the number of galaxies as a function of the distance $\langle N_{gal}(r) \rangle$. The Sloan Digital Sky Survey data shows that the function $\langle N_{gal}(r) \rangle$ becomes constant for $r \gtrsim 100$ Mpc (which corresponds to red shift $z \sim 0.02$) (see e.g. Joyce et al. (2005)). Therefore, an instrument with the field of view (FoV), which encompasses the volume $\sim (100 \text{ Mpc})^3$ at distances, corresponding to $z \lesssim 1$, will observe homogeneous matter distribution. Let us take Hubble distance as an estimate for such distances: $H_0^{-1} \sim 3.8 \times 10^3$ Mpc (here H_0 is a present day Hubble constant). Then the minimal FoV θ_{fov} is determined from a simple relation $\theta_{fov}^2 H_0^{-3} \gtrsim (100 \text{ Mpc})^3$, i.e. $\theta_{fov} \gtrsim 15'$. The FoV of XMM-Newton is precisely of this order $\theta_{xmm} \sim 30'$. Therefore, the strongest signal from small z can be missed if only “empty fields” are selected for the XMM XRB observations.

However, wide field-of-view instruments or the instruments which have conducted all-sky surveys, like HEAO-1 or ROSAT cannot miss the largest contribution to the DM decay signal from $z < 10$ because of the full sky coverage. Thus, the above argument should be used in a reverse sense: to find the DM decay signal it is necessary to use the data on the X-ray background collected from the whole sky, rather than from the “deep field” observations of a narrow-field instrument.

3 RESTRICTIONS ON PARAMETERS OF STERILE NEUTRINOS FROM THE MEASUREMENTS OF THE DIFFUSE X-RAY BACKGROUND

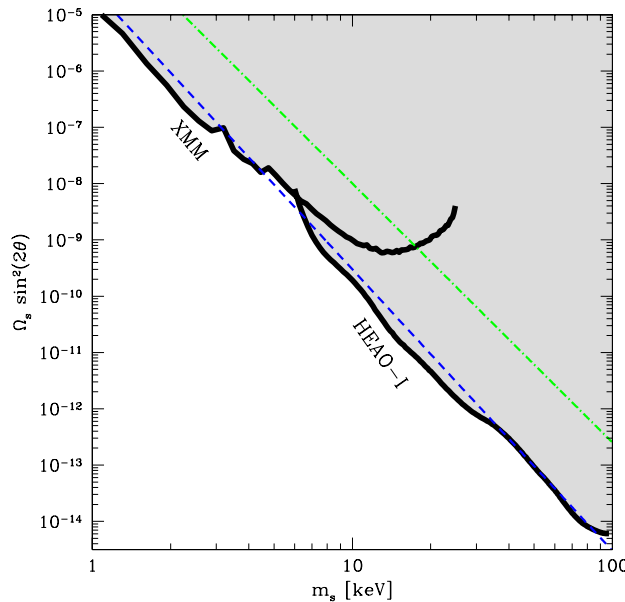


Figure 2. Exclusion plot on parameters m_s and $\sin^2 2\theta$ using HEAO-1 and XMM data. The values in the non-shaded region are allowed. In the region where both HEAO-1 and XMM-Newton data is available, HEAO-1 provides a more stringent constraint (as discussed in Section 3.2). We suppose that sterile neutrino constitute 100% of all the DM. (i.e. $\Omega_s = \Omega_{DM}$). To remove dependence on the value of Ω_{DM} , we choose to plot $\Omega_s \sin^2 2\theta$ rather than $\sin^2 2\theta$. The results can be described by a simple empirical formula Eq.(6) (thin blue dashed line on the Figure). The dash-dotted green line represent exclusion region, obtained if one attributes all 100% of the XRB flux to DM at energies $E \lesssim m_s/2$.

3.1 Restriction from HEAO-1 measurements

The above analytical approximation (5) provides a good fit to the HEAO-1 data. No DM decay feature with the spectrum of the form of (3) (corrected for the spectral resolution of the instrument) is evident in the data. Straightforward constraint on the possible contribution of DM decays into the XRB spectrum is that the flux of the DM decay contribution does not exceed the total flux. Such an approach was used by Dolgov & Hansen (2002), who applied it to the broad-band XRB model of Ressel & Turner (1989). Using the fit (5) of Gruber et al. (1999), which gives a much better description in the keV region, we obtain an exclusion curve, shown as green dash-dotted line on Fig. 2.

Clearly this restriction is model independent and rigorous. However, it can be made stronger. Indeed, the experimentally measured XRB background is monotonic at energies from keV to GeV (see Gruber et al. (1999)). If the flux of the DM have composed significant part of all XRB, contributions to XRB, *unrelated* to the radiative DM decay, should have combined themselves into a spectrum with a sudden narrow “dip”. In particular, at energies $E \geq m_s/2$ some new physical phenomena should have suddenly “kicked in”, causing the spectrum to experience a very sharp “jump”. Moreover, the form of this dip must have been almost the same as the dark matter contribution with a minus sign. This would have required a mechanism of a very precise fine-tuning of contributions to XRB between DM and various physical phenomena or simply a chance coincidence. Of course, such a conspiracy cannot be absolutely excluded, in particular because of the lack of unambiguous theoretical predictions of the shape of XRB spectrum.

However, it is very unlikely to have a precise cancellation of contributions of different nature. So, in what follows we will assume that such a situation does not happen (in particular, this does not happen in models, attributing existing XRB shape to AGN emissions (Worsley et al. (2005); Treister & Urry (2005))).

Therefore, in the present work we argue that the constraint on the possible DM contribution to the XRB resulting from HEAO-1 data can be improved using the statistical analysis of the data. Our strategy will be the following. We take the actual HEAO-1 data and fit it to the model of the form (5) (varying C_{XRB} , T_{XRB} , Γ_{XRB}) plus an additional DM flux (3) (corrected for the spectral resolution of HEAO-1 instrument). Addition of a large DM contribution would worsen the quality of the model fit to the data, while addition of a small DM contribution does not change the overall fit quality. Thus, one can put a restriction on the DM contribution by allowing the DM component to worsen the fit by a certain value. Taking into account that we have around 40 degrees of freedom of the system under consideration, we take the maximal allowed value of the reduced chi square of the fit to be $\chi^2 < 3$. Thus on technical level our method restricts the flux of DM to be of the order of errors of measured XRB flux, rather than its total value.

The results of the application of the above algorithm to the data are shown on the Fig. 2. The allowed values of $(m_s, \Omega_s \sin^2 2\theta)$ are those in the unshaded region.⁴ The shaded region below the dash-dotted line is excluded under the assumption that XRB spectrum does not have an unknown feature (a “dip”), fine-tuned to be located precisely at energies where DM contributes.

According to Eqs. (3)–(4) flux of DM is proportional to $\Omega_s \sin^2 2\theta$. Therefore we choose to plot this value rather than conventional $\sin^2 2\theta$ on y axis of Fig. 2. This removes uncertainty, related to the determination of Ω_{DM} . Notice, that the results obtained from HEAO-1 data (thick solid lines on Fig. 2) are model independent and can be applied to any DM candidate, which has a decay channel into a lighter particle and a photon, with its decay width Γ related to $\sin \theta$ via Eq. (4).

3.2 Restriction from XMM background measurements

In the energy band below 10 keV the XRB was studied by numerous narrow FoV instruments, including XMM-Newton. Better angular resolution and sensitivity of these instruments has enabled to resolve some 90% of the XRB into point sources (Brandt & Hasinger (2005); De Luca & Molendi (2005); Bauer et al. (2004)). Apparently, better sensitivity should enable to put tighter constraints on the possible DM contribution into the XRB. However, in this section we show that this is not the case.

The key point which leads to such a conclusion is that the better sensitivity (to point sources) of these instruments is achieved due to the better angular resolution, rather than due to the increase of the effective collection area. Thus, if one is interested in the diffuse sources, the sensitivity is not improved compared to HEAO-1. On the contrary, in the narrow FoV instruments the XRB signal is collected from a smaller portion of the sky, which leads to lower

⁴ The normalization of XRB spectrum, measured by HEAO-1, is known to be lower than any other XRB measurements (Gilli (2003); Moretti et al. (2003)). Therefore on Fig. 2 HEAO-1 data were *increased* by 40% according to De Luca & Molendi (2005); Worsley et al. (2005); Treister & Urry (2005) (see, however Gilli (2003)). This weakens the restriction of Fig. 2 by about 10%, as compared to actual HEAO-1 data.

statistics of the signal. At the same time, the instrumental background (which is thought to be due to the cosmic rays hitting the instrument) is roughly the same for narrow and wide field instruments. Thus, the ratio of the counts due to the photons of the XRB to the instrumental background counts is smaller for the narrow field instruments and one needs larger integration times to achieve good statistical significance of the XRB signal.

The above problem would not have affected the constraints on m_s , $\sin \theta$ if they were imposed by the condition for the flux in the DM decay component not to exceed the total XRB flux in a given energy interval. However, as the statistical significance of the XRB signal in the narrow FoV instruments is lower, bigger errors decrease χ^2 value, and therefore the imposed limit on DM will be worse than that of the corresponding wide FoV instruments.

The exclusion plot in the $(m_s, \Omega_s \sin^2 2\theta)$ parameter space obtained from the analysis of the XMM data, is shown in Fig. 2. We took the actual data of two collections of XMM background observations (Lumb et al. (2002), total exposure time ~ 450 ksec and Read & Ponman (2003) total observation time ~ 1 Msec). The form of the XMM background is fitted by the power-law with the index $\Gamma = 1.4$ (Lumb et al. (2002)), in agreement with Eq. (5). Applying to XMM data our method, as described in the previous Section, we find the restrictions, shown on Fig. 2. In the neutrino mass region $6 \text{ keV} \lesssim m_s \lesssim 20 \text{ keV}$ where both HEAO-1 and XMM data are available, the XMM-Newton background provides weaker restriction that the data from HEAO-1, because of the reason discussed above (the XMM FoV has the radius $15'$, which is much smaller than that of the HEAO-1, $\sim 3^\circ$ for A2 HED detectors). In case of XMM the statistical error at energies above roughly 7 keV is dominated by instrumental background, while in case of HEAO-1, the errors at these energies were dominated by diffuse X-ray background. As a result, errors of flux determination are smaller for HEAO data, thus providing more stringent restrictions. Of course, the XMM data provides the constraints on parameters of the neutrino in the region $1 \lesssim m_s \lesssim 6 \text{ keV}$ where HEAO-1 data are not available. The data on Fig. 2 fits to the simple empirical formula:

$$\Omega_s \sin^2(2\theta) < 3 \times 10^{-5} \left(\frac{m_s}{\text{keV}} \right)^{-5}. \quad (6)$$

3.3 Discussion.

In this work we have looked for signatures of sterile neutrino decay in the extragalactic X-ray background. The main result of our paper is the plot on Fig. 2 which constraints the properties of sterile neutrino as a dark matter candidate.

Let us compare our exclusion plot with the similar plots, found in other works. Dolgov & Hansen (2002) used a broad-band limit, put on XRB by Ressel & Turner (1989), to find a restrictions on sterile neutrino parameters. First of all, in the keV energy band the limit of Ressel & Turner (1989) is weaker than that of Gruber et al. (1999), which we are using in this paper. Therefore the dashed-dotted line on the Fig. 2 provides model-independent restrictions on parameters of sterile neutrino that are stronger than the similar bound on Fig. 4 in Dolgov & Hansen (2002). Second, as discussed in Section 3, we put a restriction on parameters of sterile neutrino, based on the statistical analysis of the actual experimental data of HEAO-1 and XMM-Newton missions. Such a constraint is possible under the assumption that there is no extremely unlikely fine-tuning between various components, contributing to the XRB. To put it differently, the observed XRB spectrum is monotonic in keV range (at energies below ~ 15 keV it was checked by various X-ray

missions, including recent measurements by XMM and Chandra). Therefore, we assume that XRB spectrum *without* DM has no “dip” with the shape and location precisely at the place, where DM contributes. The results of our analysis are shown in thick black solid line on Fig. 2. As the statistical quality of the data is good, this puts about two orders of magnitude stronger restrictions than those, represented by the dashed-dotted line. Region between the solid (or its empirical fit, Eq. (6)) and dashed-dotted lines is excluded under the assumptions discussed above.

Abazajian et al. (2001b) provide an exclusion plot (also quoted by Abazajian (2005)) based on potential observations of the Virgo cluster with *Chandra* ACIS instrument. This plot represents a theoretical prediction (rather than the processing of actual *Chandra*’s data) based on analysis of *Chandra*’s instrumental background and on certain model of Virgo cluster. We plan to analyze the observations of clusters of galaxies with various X-ray satellites to see whether in this way one can obtain stronger constraints. The results will be published elsewhere.

We would like to stress once again, that one cannot really put a model-independent restrictions on the mass of sterile neutrino m_s , as the relation between the mass of sterile neutrino, the mixing angle and the present-day sterile neutrino density Ω_s is essentially unknown (changes, depending on the model). Therefore presently there exists no robust upper limits on the mass of sterile neutrino from astrophysical observations.

The results of this work show that a possible strategy to look for a feature of DM decay in the XRB is to use data of “all sky surveys” rather than “deep field observations” and utilize instruments with the largest possible FoV (rather than best angular/spectral resolution). An example of such an instrument can be INTEGRAL, which currently plans an observation of XRB.

Acknowledgements

We would like to acknowledge useful discussions with A. Kusenko, I. Tkachev and R. Rosner. This work was supported in part by the Swiss Science Foundation and by European Research Training Network contract 005104 “ForcesUniverse”.

REFERENCES

- Abazajian K., Fuller G.M. and Patel M., 2001a, Phys. Rev. D **64**, 023501.
- Abazajian K., Fuller G.M. and Tucker W.H., 2001b, Ap.J. **562**, 593.
- Abazajian K., 2005, astro-ph/0511630
- Ahmad Q. R. et al., 2002, Phys. Rev. Lett. **89**, 011301.
- Asaka T., Blanchet S. and Shaposhnikov M., 2005, Phys. Lett. B **631**, 151.
- Asaka T. and Shaposhnikov M., 2005 Phys. Lett. B **620**, 17.
- Barger A. J., 2003, Rev. Mex. AA Ser. Conf. **17**, 226.
- Barkovich, M., D’Olivo, J. C., & Montemayor, R. 2004, Phys. Rev. D **70**, 043005.
- Bauer F. E. et al., 2004, AJ **128**, 2048.
- Brandt W.N. and Hasinger G., 2005, ARA&A, **43**, 827.
- De Luca A. and Molendi S., 2004, A&A **419**, 837.
- Dodelson S. & Widrow L.M., 1993, Phys. Rev. Lett. **72**, 17
- Dolgov A.D. and Hansen S.H., Astropart. Phys., 2002, **16**, 339.
- Eguchi K. et al. [KamLAND Collaboration], 2003 , Phys. Rev. Lett. **90**, 021802
- Fryer C.L. and Kusenko A., 2005, astro-ph/0512033.

Fukuda Y. et al. [Super-Kamiokande Collaboration], 1998, Phys. Rev. Lett. 81, 1562.

Fukugita M. and Yanagida T., 1986, Phys. Lett. B **174**, 45.

Fuller, G. M., Kusenko, A., Mocioiu, I., & Pascoli, S. 2003, Phys. Rev. D **68**, 103002.

Gell-Mann M., Ramond P. and Slansky R., in *Supergravity*, eds. P. van Nieuwenhuizen and D. Z. Freedman (North Holland, Amsterdam 1980).

Gilli R., Invited talk at COSPAR X-ray Session: New X-ray Results from Clusters of Galaxies and Black Holes, Houston, Texas, 10-12 Oct 2002 [arXiv:astro-ph/0303115].

Glashow S.L., 1979, in *Proc. of the Cargese Summer Institute on Quarks and Leptons*, Cargese, July 9-29, eds. M. Levy et. al (Plenum, 1980, New York), p707.

Gruber D.E., Matteson J.L., Peterson L.E. and Jung G.V., 1999, Ap. J. **520**, 124.

Joyce M., Sylos Labini F., Gabrielli A., Montuori M. and Pietronero L., 2005, A&A, **443**, 11.

Kusenko A. and Segre G., 1997, Phys. Lett. B, **396**, 197 .

Kuzmin V.A., Rubakov V.A. and Shaposhnikov M. E., 1985, Phys. Lett. B **155**, 36.

Mapelli M. and Ferrara A., 2005, Mon. Not. Roy. Astr. Soc. **364**, 2

Marshall F. et al., 1980, Astrophys. J. **235**, 4.

Masso E. and Toldra R., 1999, Phys. Rev. D **60**, 083503.

Minkowski, P. Phys. Lett. B **67**, 421 (1977).

Mohapatra R.N. and Senjanovic G., 1980, Phys. Rev. Lett. **44**, 912.

Moretti A., Campana S., Lazzati D. and Tagliaferri G., 2003, Astrophys. J. **588**, 696.

Lumb D.H., Warwick R.S., Page M. and De Luca A., 2002, A&A **389**, 93.

Olive K.A. and Turner M.S., 1982, Phys. Rev. D **25**, 213.

Overduin J.M. and Wesson P. S., 2004, Phys. Rept. **402**, 267.

Ramond P., 1979, in Talk given at the Sanibel Symposium, Palm Coast, Fla., Feb. 25-Mar. 2 preprint CALT- 68-709 (retroprinted as hep-ph/9809459).

Read A.M. and Ponman T.J., 2003, A&A, **409**, 395. 04147;

Ressel M.T. and Turner M.S., 1989, Comments Astrophys., **14**, 323.

Revnivtsev M., M. Gilfanov, R. Sunyaev, K. Jahoda and C. Markwardt, Astron. Astrophys. **411**, 329 (2003).

Revnivtsev M., Gilfanov M., Jahoda K. and Sunyaev K., 2005, A&A **444**, 381.

Shi X.D. and Fuller G.M. 1999, Phys. Rev. Lett. 82, 2832.

Treister E. and Urry C.M., 2005, Ap. J. **630** 115.

Viel M., Lesgourges J., Haehnelt M.G., Matarrese S and Riotto A., 2005, Phys. Rev. D 71, 063534

Worsley M.A. et al., 2005, Mon. Not. Roy. Astr. Soc. **357**, 1281.

Yanagida T., 1979, In *Proceedings of the Workshop on the Baryon Number of the Universe and Unified Theories, Tsukuba, Japan, 13-14 Feb*; 1980, Prog. Theor. Phys. **64**, 1103.

Zdziarski A.A., 1996, Mon. Not. Roy. Astr. Soc. **281**, L9.